Pergamon

0038-092X(95)00025-9

Solar Energy Vol. 55, No. 1, pp. 21–27, 1995

0038-092X/95 $9.50 + 0.00

INVESTIGATION OF MINUTE SOLAR RADIATION DATA

R. A. GANSLER, S. A. KLEIN and W. A. BECKMAN
Solar Energy Laboratory, University of Wisconsin-Madison, Madison, WI, U.S.A.

Abstract—Simulation studies of solar energy systems have traditionally been performed using hourly data because data for shorter time periods are generally unavailable for extended periods. If simulations using hourly data are to provide accurate results, the variation of radiation within an hour must have a negligible effect on a system's performance. This paper examines minute radiation data from three locations. The distribution of minute data within the hour is found to differ from previously presented distributions of daily radiation in a month. Comparisons of calculated and measured minute radiation on a tilted surface show significant differences which are attributable to inaccurate estimates of the magnitude and distribution of diffuse radiation on a minute basis. Even with the same tilted surface radiation, significant differences in simulated performance using hourly and minute-by-minute data are found to exist for a simple photovoltaic system.

1. INTRODUCTION

Simulation studies of solar energy systems have traditionally used hourly meteorological data. Hourly data are appropriate for systems that respond slowly or linearly to changes in solar radiation. However, large variations in solar radiation can occur within the space of an hour and these variations could lead to inaccurate estimates of system performance if based on hourly data. Variations of radiation within an hour have been typically estimated by one of three methods: linear interpolation between two hourly values, following the variation of extraterrestrial radiation, or assuming uniform irradiation during the hour. The solar radiation data available on a minute-by-minute basis are quite limited, but sufficient data are available to indicate the importance of using short-term data in modeling studies.

The variation of radiation data on a minute basis can be represented in terms of a cumulative frequency distribution (CFD) such as those proposed by Liu and Jordan (1960) and Bendt *et al.* (1981) for the distribution of daily and hour radiation within a day. Suehrcke (1988) and Suehrcke and McCormick (1989) have proposed a CFD for minute radiation based on data for Perth, Australia, which is markedly different from the Liu and Jordan CFD. Suehrcke's CFD has a bimodal shape. Suehrcke provides an explanation for this behavior and has derived a mathematical model to represent the bimodal shape of the CFD for minute data. Skartveit and Olseth have investigated the statistical characteristics of short-term radiation data at three locations (Atlanta, Ga. San Antonio, Tex., and Geneva, Switzerland). They also have found instantaneous and 5-min data to have a more bimodal distribution that the corresponding hourly averages. Their analysis differs from that of Suehrcke and the present study in that their clearness indices are defined relative to clear sky, rather than extraterrestrial radiation.

Minute radiation data for three U.S. locations were available through the U.S. Department of Energy SEMRTS (Solar Energy Meteorological Research and Training Site Program). The three locations and time periods are Atlanta, Ga (lat 33.6°, Jan.–Dec., 1981), San Antonio, Tex. (lat 29.5°, Apr. 1981–Mar., 1982) and Albany, NY (lat 42.7°, Aug. 1980–Jul., 1981). These data were collected by Georgia Institute of Technology, Trinity University, and State University of New York, respectively. The yearly-average clearness indices and ambient temperatures for Atlanta, San Antonio and Albany are, respectively (0.50, 16°C), (0.53, 20°C) and (0.42, 8.7°C).

Figures 1–3 show the CFDs for data collected for 1 year in Atlanta for three airmass groupings,

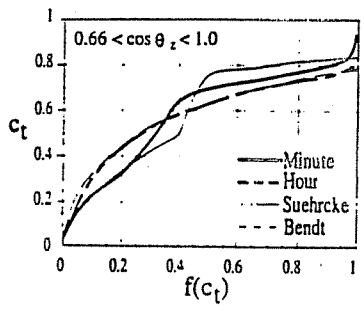

Fig. 1. Cumulative frequency distribution at low airmass. Atlanta.

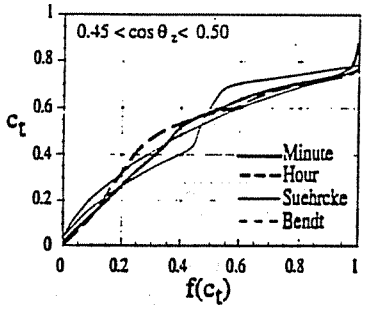

Fig. 2. Cumulative frequency distribution at intermediate airmass, Atlanta.

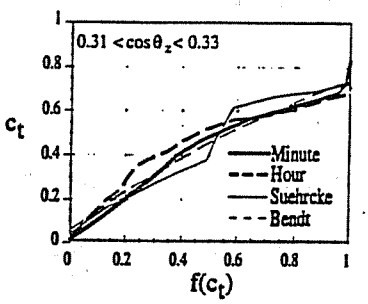

Fig. 3. Cumulative frequency distribution at high airmass, Atlanta.

represented in terms of zenith angle. On a minute basis, the CFD is a plot of the minute clearness index, c_t, versus $f(c_t)$, the fraction of the total time the clearness index was above that value. The minute clearness indices, c_t, were calculated from

$$c_t = G/G_0 \tag{1}$$

where G is the measured minute terrestrial solar flux and G_0 is the minute extraterrestrial solar flux. Only the minutes falling within the indicated zenith angle range were used in constructing the CFD curves. An hourly clearness index, k_t, was determined by summing the minute data in each hour. Also shown in Figs 1–3 are the CFDs for the hourly data (with the hourly clearness index, k_t replacing c_t) and the analytical CFDs developed by Bendt *et al.* (1981) for daily radiation and Suehrcke (1988) corresponding to the average hourly clearness index.

There is some evidence of bimodality at lower airmasses for the minute data but this effect decreases with increasing airmass. The bimodality indicates, that, on a minute basis, there is higher probability for low or high values of solar radiation with fewer intermediate values. The hourly CFD curves closely agree with the Bendt *et al.* (1981) distribution. Skartveit and Olseth (1992) considered the effect of airmass by defining the clearness index as the ratio of the measured radiation to the clear-sky radiation for the same period. The results in Figs 1–3 tend to indicate that the effect of airmass on the minute radiation distributions cannot be completely accounted for by defining the clearness index in this manner.

It would be convenient if the distribution of minute clearness indices within an hour were well-represented by the distribution of daily radiation within a month given by Liu and Jordan (1960) and Bendt *et al.* (1981). However, the distributions of c_t do not seem to exhibit the same behavior. CFDs of the minute data were developed in several ways, for example, using only those hours having an average clearness index within a small specified range (Gansler, 1993). Regardless of how they were determined, however, the distributions of the minute radiation data differed significantly from those for hourly data. There is, however, a consistent behavior for the c_t distributions.

The shapes of the minute clearness index distributions are similar to those of the relative humidity curves plotted by Erbs (1984) using a Weibull distribution. Using data from San Antonio and Atlanta, a two-parameter model for the c_t distributions was fit to the minute data for values of k_t from 0.3 to 0.7. The resulting correlation is:

$$f(c_t) = \frac{1 - \exp(-(c_t/\theta_1)^{\theta_2})}{1 - \exp(-(1/\theta_1)^{\theta_2})} \tag{2}$$

$$\theta_1 = 0.223 + 2.21k_t - 1.211k_t^2 \tag{3}$$

$$\theta_2 = 5.948 \times 10^{-9}\, e^{30.054k_t} + 1.587\, e^{1.815k_t} \tag{4}$$

A comparison of the correlation (eqns 2–4) and the CFDs determined from data in the three locations appears in Fig. 4. The model represents the CFD of the minute data more closely than does the daily radiation distribution of Bendt *et al.* (1981).

Equations (2–4) were generated from an annual series of data from each location. In using all of these data, any seasonal variations would be masked. In addition, there is likely to be some variation with time of day which also cannot be seen in Fig. 4. The effect of season and time of day were considered by grouping the minute data in airmass bins for all three

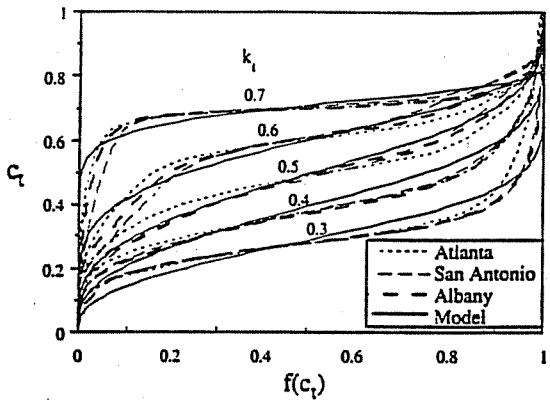

Fig. 4. CFD of minute clearness indice.

locations. Three airmass ranges were considered: (1.0–1.5), (2.0–2.5), and (3.0–3.5). Figures 5–7 show the results of c_t distributions about k_t as a function of hourly airmass.

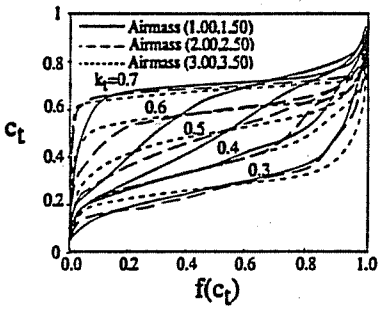

Fig. 5. CFD of minute clearness indices, Atlanta.

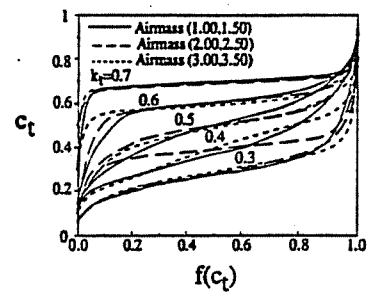

Fig. 6. CFD of minute clearness indices, Albany.

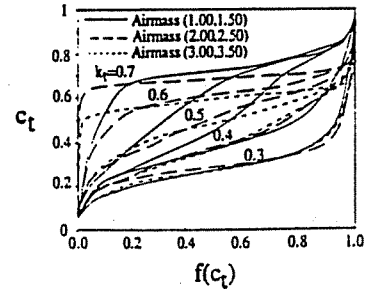

Fig. 7. CFD of minute clearness indices, San Antonio.

At both low and high hourly clearness indices, the curves exhibit little dependence on airmass. For Albany, there is virtually no difference in the distribution curves for different airmasses. The curves for all airmass values are nearly identical. However, for the other two locations, there are noticeable differences around k_t of 0.4–0.6. At low airmass, the distributions differ markedly from those of higher airmass. In fact, the distributions at low airmass are very much like a Bendt distribution. This apparent discrepancy has a possible physical explanation. At high airmass, there is a great deal of intervening sky between the observer and the sun. In order to have an intermediate value of k, the sky will be relatively uniform in terms of clouds. However, at low airmass, there can be much more of a range of minute clearness indices to give the same hourly value. The CFD model proposed in eqns (2–4) depends only on the hourly clear index. It is apparent that, for some locations, the CFD model should include a dependence on airmass as well.

2. DIFFUSE RADIATION CALCULATIONS

An initial investigation revealed that the hourly tilted surface radiation estimated using interpolated hourly average horizontal radiation values was higher than the estimated using the measured minute horizontal radiation values. This difference occurred in spite of the fact that the hourly data were constructed by summing the minute data so that the hourly horizontal radiation for the minute and hourly average data sets were identical.

The tilted surface minute radiation, G_T, was calculated as the sum of beam, diffuse, and ground-reflected contributions. To estimate the tilted surface radiation, it is necessary to first estimate the beam and diffuse radiation on a horizontal surface each minute. An analysis was undertaken to determine whether the diffuse fraction estimated using the hourly-average data would differ from that estimated using the minute data. Three diffuse fraction models, Boes *et al.* (1976), Erbs *et al.* (1982), and Reindl *et al.* (1990) were investigated. The diffuse fraction models are polynomial expressions in k_t developed from hourly measurements. The hourly diffuse radiation was calculated from

$$I_{d.hour} = ID(k_t) \tag{5}$$

where $D(k_t)$ is the hourly diffuse fraction. The

hourly total of the minute diffuse radiation was determined from

$$I_{d.min} = \sum_{i=1}^{60} G_i D(c_{t,i}) \quad (6)$$

where $c_{t,i}$ is the minute clearness index for minute i and $D(c_t)$ is the minute diffuse fraction calculated using the diffuse fraction models with those used in place of k_t. The normalized difference in the hourly diffuse radiation calculated using the minute and hourly data was quantified as a function of the hourly clearness index as indicated in eqn (7). N is the number of hours in the year having a clearness index in the interval between between $k_1 - 0.04$ and k_t.

$$\text{Error}(k_t) = \frac{1}{N} \sum_{N} \frac{I_{d.hour} - I_{d.min}}{I_{d.hour}} \quad (7)$$

Results are shown in Figs 8 and 9 for Atlanta and San Antonio, respectively. There may be an airmass dependence in the errors, but this effect was not investigated. The figures show that there can be significant error resulting from the use of hourly diffuse correlations to estimate minute diffuse radiation and the error is a function of the clearness index. This conclusion is in agreement with the findings of Suehrcke and McCormick (1988) based on radiation data for Perth, Australia.

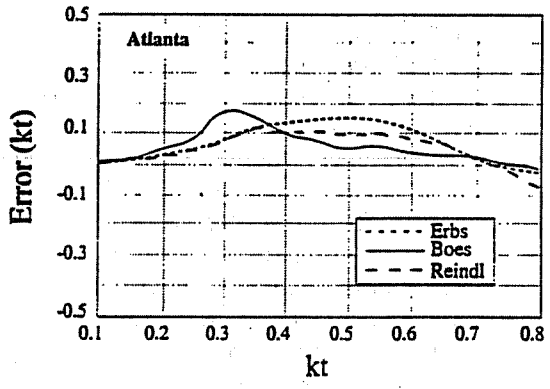

Fig. 8. Average hourly error in calculating diffuse radiation, Atlanta.

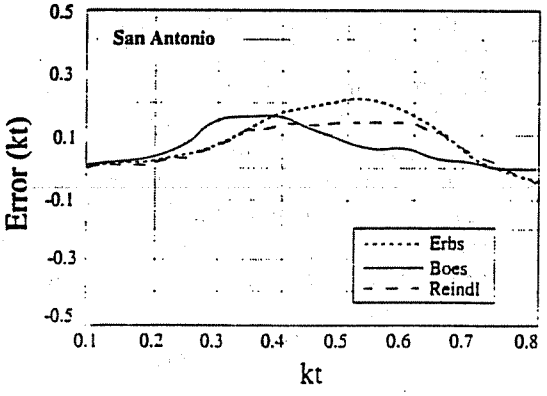

Fig. 9. Average hourly error in calculating diffuse radiation. San Antonio.

3. TILTED SURFACE CALCULATIONS

The calculation of radiation on a tilted surface requires a model for the distribution as well as the magnitude of diffuse radiation. Measurements of the diffuse radiation on a horizontal surface and the global radiation on a surface at a tilt equal to latitude were available on a minute basis. Comparisons were made between the measured and the calculated tilted surface minute radiation values. The measured horizontal diffuse and total radiation were used in these calculations to avoid confounding the results with inaccurate horizontal diffuse radiation estimates. Four diffuse distribution models were investigated: isotropic; Hay and Davies (1980); Reindl (1990); and Perez *et al.* (1988). The ground reflectance was assumed constant at a value of 0.20. A normalized error was calculated as a function of minute clearness index as indicated in eqn (8).

$$\text{Error}(c_t) = \frac{1}{N} \sum_{N} \frac{G_{T,model} - G_T}{G_T} \quad (8)$$

where, in this case, N is the number of hours in each month for which the minute clearness index was in the interval between between $c_t - 0.04$ and c_t. The normalized error in calculated tilted surface radiation for January and June in San Antonio is shown (Figs 10 and 11) as a function of the minute clearness index. All of the models show large errors in January and much smaller errors in June. The conclusion from these comparisons is that both the correlations developed to estimate the magnitude and the distribution of diffuse radiation based on hourly measurements may not be accurate when applied to data on a minute basis.

4. PHOTOVOLTAICS AND MINUTE RADIATION

Minute clearness index distributions differ from hourly clearness index distributions and they are dependent on the hourly clearness index and air mass. The logical question is how these differing distributions affect the energy output of a solar system. Simulations of space and water heating systems have typically

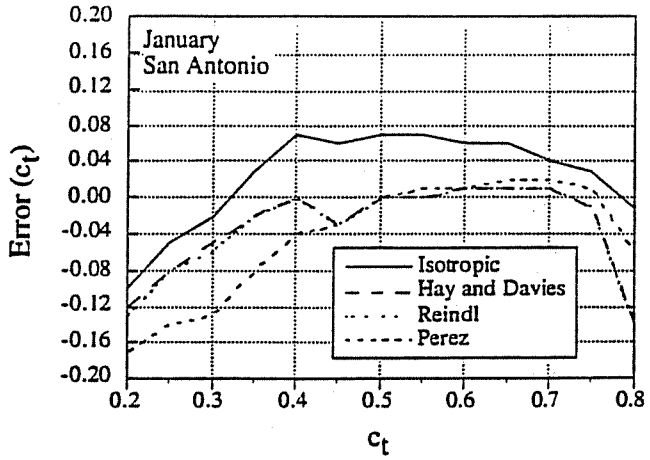

Fig. 10. Error in calculated minute tilted surface radiation for January in San Antonio using measured horizontal diffuse with four diffuse distribution models.

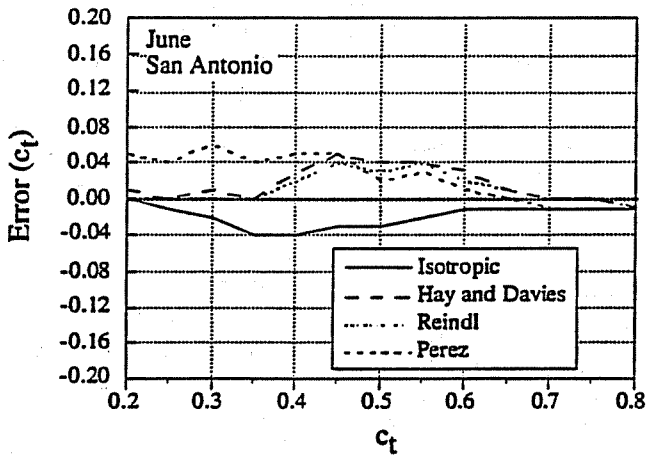

Fig. 11. Error in calculated minute tilted surface radiation for June in San Antonio using measured horizontal diffuse with four diffuse distribution models.

ignored the effects of radiation variations within an hour. The thermal capacitance effects inherent in a flat-plate solar collector would likely damp out the short-term variations in solar radiation. The time response of a photovoltaic (PV) system is, however, very fast so that the variation of radiation within an hour could be significant. Photovoltaic array output is also a non-linear function of solar radiation and cell temperature. The cell temperature is affected by the irradiation, the ambient temperature, and the power output. The relationship between power output and cell temperature is implicit, and both are related in a highly non-linear way to ambient temperature and irradiation. With all of this non-linearity, the choice of inputs used to evaluate the performance of a photovoltaic system could be important.

The magnitude of the error resulting from the use of hourly average weather data as compared to actual minute weather data has been determined by simulating a photovoltaic system. Equations describing the current–voltage characteristics of a PV cell as a function of solar radiation and ambient temperature are given in Duffie and Beckman (1991). Current–voltage characteristics can also be used to describe the electrical load. These equations were simultaneously solved using the EES program (Klein and Alvarado, 1992).

The first system investigated was a maximum power point tracking system with a 0.5 m^2 PV array. The performance of this system was simulated for October 1, 1981 using the San Antonio minute data. The simulations were also done on an hourly basis using the sum of the minute

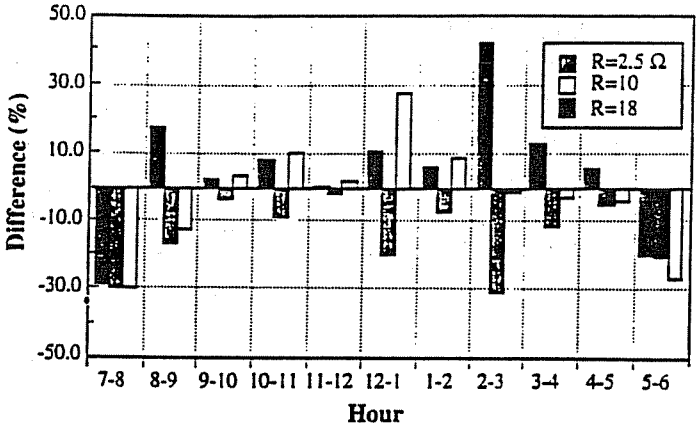

Fig. 12. Difference in electrical energy with hourly and minute simulations for a constant resistive load.

data for each hour. The difference in hourly electrical energy for this maximum power point tracking system calculated with eqn (9) were very small.

$$\text{Difference} = \frac{\text{electricity using } k_t - \text{electricity using } c_t}{\text{electricity using } c_t}. \quad (9)$$

A second system investigated represented a constant load resistance directly connected to the same 0.5 m² PV array with no battery storage. Although this photovoltaic system may not have practical applications, it clearly illustrates the effect variations in short-term radiation can have on system performance. Figure 12 depicts the results of these 1-day simulations. At a load of 10 Ω, the hourly average method works quite well, except at 12 – 1. However, at low resistance, the use of hourly average values consistently underpredicts the system performance. At a high resistance, the use of hourly average values also performs poorly but in a surprising manner. In this case, the system performance was overpredicted. This was completely unexpected because a utilizability analysis on the irradiation would indicate that minute weather should always give a higher performance, as suggested by Klein and Beckman (1984). The non-uniformity of minute radiation values would yield higher utilizability over that of the hourly average. Thus, it would seem impossible for the hourly average values to exhibit higher performance.

The explanation for these results can be seen by examining a voltage power plot. These curves are displayed in Fig. 13 for various insolation levels (250, 500 and 750 W/m²) but all at an ambient temperature of 25°C. Also displayed are three curves describing the effect of a constant resistance (5, 10 and 20 Ω). The key is to look at the intersection of the power curves with the load curves and to compare the power output at the extreme insolation levels against that of the intermediate value. At the intermediate resistance, the power delivered at the average insolation is nearly equal to the average of the power delivered at the extreme insolation levels. At a low resistance, the average insolation indicates a lower performance than would the average of the extremes. At a high resistance, the voltage power curves draw nearer to each other as the power decreases to zero. The intersection of the average insolation curve lies much closer to the high insolation intersection than it does to the low insolation intersection. This will result in the average insolation level producing more power than the average of the extremes.

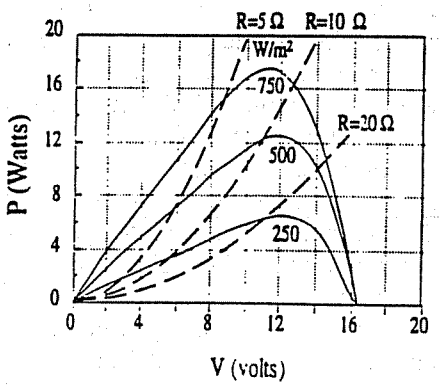

Fig. 13. Voltage–power curve of a 0.5 m² PV array, T = 25°C with resistive loads of 5, 10, and 20 W for insolation of 250, 500, and 750 W/m².

5. CONCLUSIONS

The cumulative distribution functions for minute radiation differ from those of hourly data and tend to have a bimodal shape, as noted previously by Suehrcke (1988) and Skartveit and Olseth (1992). However, some dependence on air mass is evident in the data that is not considered in the model given by eqns (2)–(4). This air mass dependence differs somewhat from that proposed in the models by Suehrcke (1988) and Skartveit and Olseth (1992) for the three U.S. locations investigated. In addition, it was found that the existing models for the diffuse fraction and distribution of diffuse radiation developed from hourly data can be inaccurate when applied to minute radiation data. The performance of solar energy systems which respond rapidly to changes in solar radiation, e.g. photovoltaic systems, may depend on the short-term variability of solar radiation. The hourly electrical energy calculated for a simple photovoltaic system using hourly data was found to be significantly different from that using minute data because of the variability of the solar radiation and the non-linear dependence of system output on radiation level.

NOMENCLATURE

c_t minute clearness index
CFD cumulative frequency distribution
D diffuse fraction for horizontal radiation
$f(c_t)$ fraction of the time clearness index is less than c_t
G minute horizontal solar radiation
G_i horizontal solar radiation for minute i within an hour
G_0 minute horizontal extraterrestrial radiation
G_T observed minute tilted surface solar radiation
$G_{T,model}$ calculated minute tilted surface solar radiation
I hourly total horizontal radiation
$I_{d,hour}$ hourly diffuse radiation on a horizontal surface calculated from I
$I_{d,min}$ hourly diffuse radiation on a horizontal surface calculated from G
k_t hourly clearness index
N number of hours of data
q_1, q_2 parameters in c_t CFD model
q_z solar zenith angle

REFERENCES

Boes E. C., Hall I. J., Praire R. R., Stromberg R. P. and Anderson H. E. Distribution of direct and total solar radiation availabilities for the U.S.A. Sandia Report SAND76-0411 (August 1976).

Bendt P., Collares-Pereira M. and Rabl A. The frequency distribution of daily insolation values. *Solar Energy* 27(1), 1–5 (1981).

Erbs D. G., Klein S. A. and Duffie J. A. Estimation of the diffuse radiation fraction for hourly, daily, and monthly-average global radiation. *Solar Energy* 28(4), 293–302 (1982).

Erbs D. Models and application for water statistics related to building heating and cooling loads. Ph.D. thesis, Mechanical Engineering Department, Univ. of Wisconsin-Madison, Madison (1984).

Duffie J. A. and Beckman W. A. *Solar engineering of thermal processes*, 2nd edn. Wiley, New York (1991).

Gansler R. A. Assessment of generated meteorological data for use in solar energy simulations. M.S. thesis, Mechanical Engineering Department, Univ. of Wisconsin-Madison, Madison (1993).

Hay J. E. and Davies J. A. Calculation of the solar radiation incident on an inclined surface. *Proceedings of the First Canadian Solar Radiation Workshop*, pp. 59–72 (1980).

Klein S. A. and Alvarado F. L. EES: Engineering equation solver. F-Chart Software, Middleton, Wis. (1992).

Klein S. A. and Beckman W. A. Review of solar radiation utilizability. *ASME J. Solar Energy Engng* 106, 393–402 (1984).

Liu B. Y. H. and Jordan R. C. The interrelationship and characteristic distribution of direct, diffuse and total solar radiation. *Solar Energy* 4(3) (1960).

Perez R., Stewart R., Seals R. and Guertin T. The development and verification of the Perez diffuse radiation model. SANDIA Report SAND88-7030, Sandia National Laboratories, Albuquerque, N.M. (1988).

Reindl D. T., Beckman W. A. and Duffie J. A. Evaluation of hourly tilted surface radiation models. *Solar Energy* 45(1), 9–17 (1990).

Skartveit A. and Olseth J. A. The probability density and autocorrelation of short-term global and beam irradiance. *Solar Energy* 49(6), 477–487 (1992).

Suehrcke H. The performance prediction of solar thermal systems. Ph.D. thesis, Univ. of Western Australia, Australia (1988).

Suehrcke H. and McCormick P. G. The diffuse fraction of instantaneous insolation values. *Solar Energy* 40(5), 423–430 (1988).

Suehrcke H. and McCormick P. G. The distribution of average instantaneous terrestrial solar radiation over the day. *Solar Energy* 42(4), 303–310 (1989).